Mechanism of Cu-catalyzed iododeboronation: A description of ligand-enabled transmetalation, disproportionation, and turnover in Cu-mediated oxidative coupling reactions

Matthew J. Andrews,[a‡] Ambre Carpentier,[b‡] Alexandra M. Z. Slawin,[a] David B. Cordes,[a] Stuart A. Macgregor,[b*] and Allan J. B. Watson[a*]

[a]EaStCHEM, School of Chemistry, University of St Andrews, Purdie Building, St Andrews, KY16 9ST, U.K.

[b]Institute of Chemical Sciences, Heriot-Watt University, Edinburgh, EH14 4AS, U.K.

ABSTRACT: We report a combined experimental and computational study of the mechanism of the Cu-catalyzed arylboronic acid iododeboronation reaction. A combination of structural and DFT analyses has allowed determination of the identity of the reaction pre-catalyst and the first complete description of the catalytic cycle. Key findings include a rationale for ligand stoichiometry related to key turnover events – the ligand facilitates transmetalation via H-bonding to an organoboron boronate generated in situ and ligand loss/gain is integral to the key oxidative events. These data provide a framework for understanding ligand effects on these key mechanistic processes, which underpin several classes of Cu-mediated oxidative coupling reactions.

Introduction

Cu-catalyzed iododeboronation of aryl boronic acids using iodide is a useful reaction for the synthesis of aryl iodides (Scheme 1a).[1-4] More importantly, this reaction accommodates iodide radioisotopes providing products that have important applications within in vivo imaging and radiotherapy.[5-9]

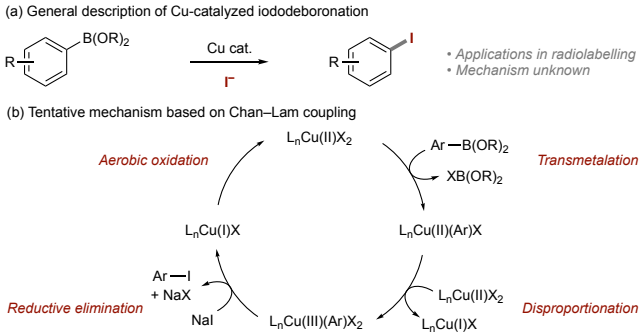

Scheme 1. (a) General representation of Cu-catalyzed iododeboronation. (b) Tentative description of the iododeboronation reaction.

There are several reported methods for Cu-catalyzed iododeboronation, each with subtle variations in copper source, ligand, and associated reaction conditions.[1-4] Related copper-catalyzed or -mediated halodeboronation reactions, such as the equivalent fluorination reaction, also operate with similar reaction conditions.[10-13] This general reaction class therefore has broad applications across synthetic chemistry and specific applications in bio-facing fields.

Very limited mechanistic information is available on the halodeboronation reaction in general, with a tentative mechanistic description of the iododeboronation largely based on the framework of the Chan–Lam reaction (Scheme 1b).[14-17] This proposed mechanism involves transmetalation of the arylorganoboron compound to Cu(II), giving a Cu(II)(aryl) species, followed by disproportionation to Cu(III), and anion exchange/reductive elimination to give the aryl iodide product and Cu(I). Aerobic reoxidation of Cu(I) to Cu(II) closes the cycle.

Despite the importance and influence that ligand stereoelectronics exert on redox processes at metal centers, robust identification of intermediate ligand structure and speciation states remains a general problem in Cu-mediated oxidative catalysis. This renders the study of key mechanistic events, such as transmetalation, disproportionation, and oxidative turnover, difficult to understand and, therefore, control through rational catalyst design.

The main knowledge in this area arises from several key studies of catalytic reactions. Hartwig identified a Cu(III) intermediate in solution and proposed a mechanism for transmetalation of arylboronic acid pinacol (ArBpin) esters in a fluorodeboronation reaction using an F^+ reagent, with ligands proposed for this key intermediate and event.[11] Stahl,[15,16] Watson,[17,18] and Schaper[19,20] proposed ligand sets for related Chan–Lam etherification and amination reactions, with broadly similar descriptions of rate-limiting transmetalation.[21] Computational analysis of Chan–Lam amination reactions have aligned closely, although with some differences in the interpretation of the rate-limiting event.[22] While integral to many Cu-based oxidative coupling reactions, there is limited information on the disproportionation event or oxidative turnover.

Here we report a detailed mechanistic description of the Cu-catalyzed iododeboronation reaction using a combination of structural, spectroscopic, and computational analyses. For the first time, this includes an assessment of ligand structure at all stages of the proposed catalytic cycle. More broadly, this analysis has provided insight into the transmetalation, disproportionation, and oxidative turnover events that underpin many Cu-mediated oxidative coupling reactions.

Results

Synthesis and characterization of Cu complexes. For our analysis, we selected a catalytic iododeboronation system reported by Gouverneur using $Cu(OAc)_2$ and 1,10-phenanthroline (phen) as the catalyst/ligand system and NaI as the requisite source of iodide (Scheme 2).[7] Based on these conditions, we sought to prepare complexes that may be formed in situ.

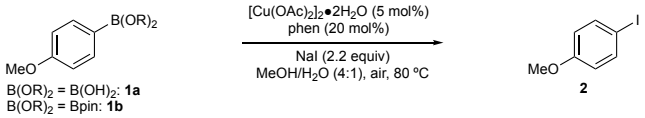

Scheme 2. Model iododeboronation system used in this study.

Treatment of $[Cu(OAc)_2]_2•2H_2O$ with phen delivered the monomeric complex $[Cu(OAc)(phen)_2]OAc$ (**[3]OAc**)[23] or the dimeric complex $[Cu(OAc)_2(phen)]_2•\mu\text{-}H_2O$ (**4**)[24] (Scheme 3a). Recrystallization of **[3]OAc** in CH_2Cl_2 fortuitously led to formation of $[Cu(OAc)(phen)_2]Cl$ (**[3]Cl**) (Scheme 3c). Treatment of $[Cu(OAc)_2]_2•2H_2O$ with phen under halodeboronation reaction conditions (NaI, $MeOH/H_2O$) led to formation of $[Cu(I)(phen)_2]I$ (**[5]I**) (Scheme 3d).[25] Crystalline material from the reaction mixture of an iododeboronation reaction of **1a** conducted under an inert atmosphere was isolated and determined to be the dimeric complex $[Cu(\mu\text{-}I)(phen)]_2$ (**6**) (Scheme 3e).[26]

Discussion

Identification of reaction-relevant Cu complexes. To elucidate the function of reaction components and identify reaction-relevant Cu complexes, $[Cu(OAc)_2]_2•2H_2O$ was first treated with NaI; however, no reaction or denucleation of the paddlewheel was observed by EPR spectroscopy (not shown, see Fig. S12).

We therefore hypothesized that the reaction initiates by formation of a $Cu(II)(phen)_n$ complex. Treatment of $[Cu(OAc)_2]_2•2H_2O$ with phen (2 equiv) and analysis by EPR spectroscopy showed formation of a complex with a spectrum consistent with that of **[3]OAc** and less consistent with **4** (Figure 1). This suggested that **[3]OAc** was the dominant species arising from reaction-relevant Cu:phen stoichiometry (1:2).

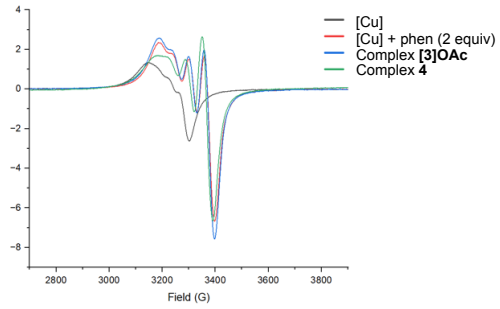

Figure 1. Overlaid EPR spectra for $[Cu(OAc)_2]_2•2H_2O$ (black), complex **[3]OAc** (blue), complex **4** (green), and the proposed in situ formation of through complexation of **[3]OAc** by treatment of $[Cu(OAc)_2]_2•2H_2O$ with phen (2 equiv) (red). Solvent = $MeOH/H_2O$ (4:1). [Cu] = $[Cu(OAc)_2]_2•2H_2O$.

Using pre-formed **[3]OAc** or **4** in the iododeboronation reaction of **1a** delivered the expected product **2**, indicating reaction relevance and catalytic competency (Scheme 4); however, while **[3]OAc** exhibited catalytic turnover, **4** did not.

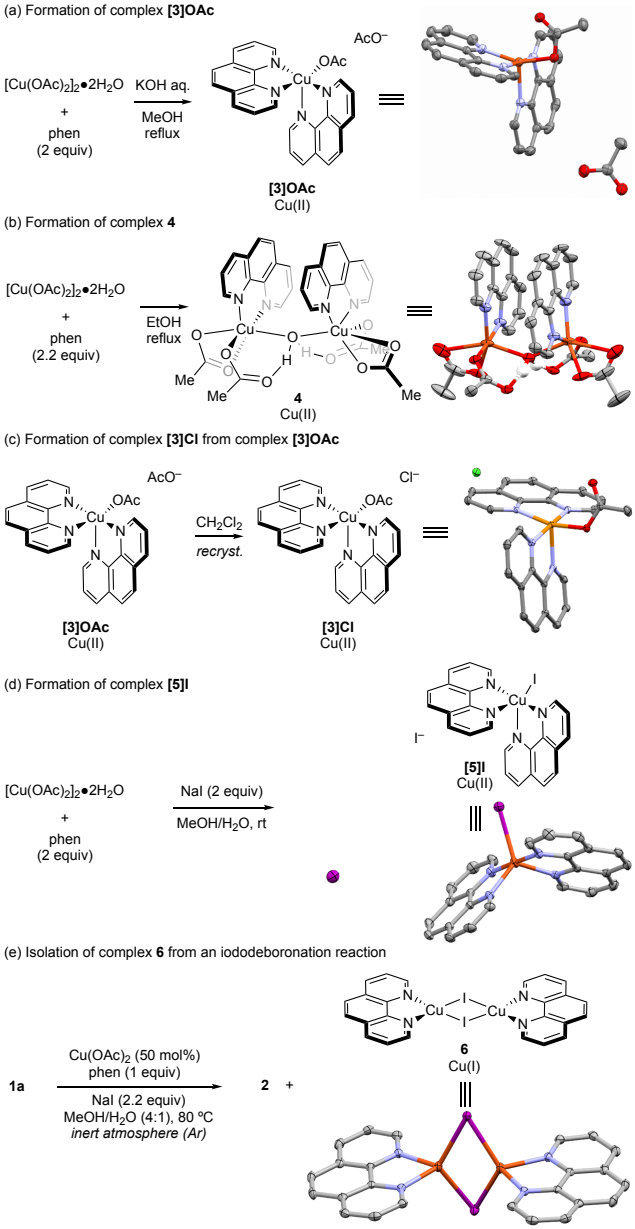

Scheme 3. Formation of Cu complexes **3-6.**

Note that to avoid complications in data analysis, **1a** was used to avoid off-cycle inhibitory processes that are associated with release of pinacol from reactions using ArBpin (i.e., **1b**; see ESI for control experiments).[17] In addition, while it is possible to prepare $Cu(II)(phen)_3$ complexes,[27] these are not readily accessible under conditions relevant to the iododeboronation process and, as such, were discounted from this study.

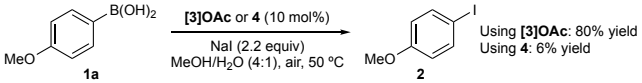

Scheme 4. Competency of **[3]OAc** and **4** in the iododeboronation of **1a.** Yields determined by ^1H NMR using an internal standard.

Treatment of $[Cu(OAc)_2]_2•2H_2O$ with phen and NaI and analysis by EPR spectroscopy revealed a solution structure consistent with complexes **[3]OAc** and **[3]Cl**, with the observation of increased line broadening, and which were significantly different

to the spectrum of **[5]I** (Figure 2). Based on these data, we propose the formation of **[3]I** in situ, which subsequently proceeds to **[5]I** via further anion metathesis. Attempts to isolate **[3]I** were unsuccessful – all attempts led to isolation of **[5]I**.

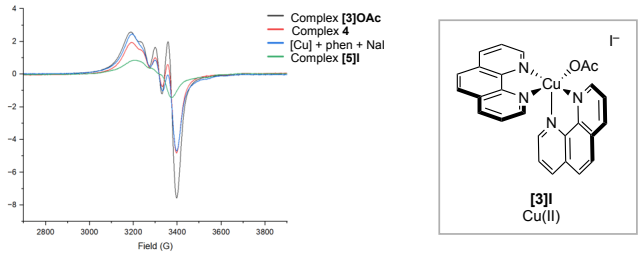

Figure 2. Overlaid EPR spectra for compound **[3]OAc** (black), complex **4** (red), complex **[5]I** (green), and the proposed in situ formation of **[3]I** through reaction of $[Cu(OAc)_2]_2 \bullet 2H_2O$ with phen (2 equiv), and NaI (2 equiv) (blue).

Use of complexes **[3]Cl** and **[5]I** in halodeboronation reactions was informative (Table 1). Stoichiometric **[3]Cl** delivered only 16% of the expected chloroarene product **7** while stoichiometric **[5]I** delivered quantitative conversion to **2** (entries 1 and 2). Similar effects were observed when using catalytic **[3]Cl** and **[5]I** in the presence of NaCl and NaI, respectively (entries 3 and 4): poor conversion was observed with **[3]Cl** but **[5]I** was competent. Interestingly, using NaI as the halide source, **[3]Cl** was catalytically competent and delivered exclusively the iododeboronation product **2** (**7** not observed) despite the presence of 10 mol% chloride (entry 5). The reciprocal reaction using **[5]I** with NaCl delivered iododeboronation commensurate with the presence of 20 mol% iodide (from 10 mol% **5**) as expected, but low levels of chlorodeboronation despite the presence of excess chloride (entry 6).

Table 1. Halodeboronation competency and halide effect of complexes **[3]Cl** and **[5]I**.

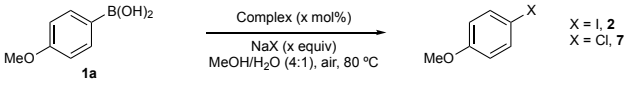

Entry	Complex (loading)	NaX (equiv)	Yield (product)[a]
1	**[3]Cl** (1 equiv)	---	16% (**7**)
2	**[5]I** (1 equiv)	---	>99% (**2**)
3	**[3]Cl** (10 mol%)	NaCl (2.2)	20% (**7**)
4	**[5]I** (10 mol%)	NaI (2.2)	83% (**2**)
5	**[3]Cl** (10 mol%)	NaI (2.2)	67% (**2**)
6	**[5]I** (10 mol%)	NaCl (2.2)	16% (**2**) 17% (**7**)

[a]Yields determined by ^{1}H NMR using an internal standard.

These data suggest that (i) **[3]Cl** and **[5]I** are catalytically competent, (ii) complex $[\mathbf{3}]^+$ is likely a key on-cycle species and exists in equilibrium with, or is a precursor to, $[\mathbf{5}]^+$, and (iii) iodide transfer is more efficient than chloride. This latter point begins to impact upon understanding of halodeboronation in general, in particular aligning with the more difficult fluorodeboronation process.[10-13]

In situ reaction monitoring and sequential addition of reagents showed productive reactivity was only observed with the addition of NaI prior to **1a** (not shown, see ESI S24, S25), suggesting transmetalation occurs after formation of complex **[3]I**. Attempts to identify Cu(II)(aryl) complexes were unsuccessful, consistent with transmetalation being rate-limiting as indicated for other reactions in this class, e.g., Chan–Lam processes.[14]

We hypothesized that Cu(I) complex **6** was produced following reductive elimination of the product from a Cu(III) intermediate. This complex was notable due to the 1:1 Cu:phen ratio, which implied loss of one phen ligand from the proposed intermediate $[\mathbf{3}]^+$. To enable catalysis, **6** would require oxidation to Cu(II) in the presence of air (the terminal oxidant used in the iododeboronation process). Oxidation of CuOAc under air was therefore monitored by UV-Vis (Figure 3a) and in the presence of other reaction-relevant additives. Oxidation was not observed in air or in the presence of NaOAc or substrate **1a**. $B(OH)_3$, which has been effective in promoting oxidation in Chan–Lam amination reactions, also had no effect;[17] however, addition of phen (Cu:phen = 1:2) and AcOH was effective at promoting the oxidation. The effect of AcOH is consistent with previous observations in Chan–Lam reactions.[15-17] The dependence on a Cu:phen ratio of 1:2 for catalyst turnover was shown by the direct use of 10 mol% **4**, when a yield of 6% was obtained. When an additional equivalent of phen was included (with respect to Cu loading), this enabled catalytic turnover, resulting in a 70% yield (Table S5). The effect of phen stoichiometry on oxidation has was notable: oxidation of [Cu(phen)I] required an 18 h reflux, compared to $[Cu(phen)_2I]$, where oxidation was achieved within 20 mins at 70 °C.[28] Heating to a minimum of 30 °C was also required for oxidation to occur (Fig. S9), with a reaction yield of 9% (i.e., one catalytic cycle) at room temperature and 70% at 30 ºC (Table S2). Moreover, the EPR spectrum of the oxidation in the presence of phen was consistent with that of the proposed **[3]I** (Figure 3b).

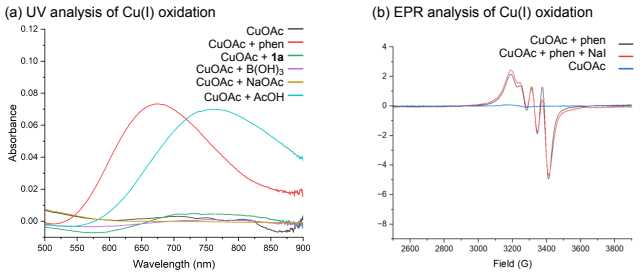

Figure 3. (a) Oxidation of CuOAc in air and in absence/presence of reaction components. (b) EPR spectra of oxidation of CuOAc + phen/NaI under air.

The above data indicated that ligand speciation, specifically relating to phen stoichiometry, varied during the reaction and Cu required one or two phen for specific mechanistic events. To shed more light on this issue and to clarify the details of the iododeboronation reaction mechanism we turned to DFT calculations (Figure 4).[29]

The geometry computed in solution for the $[Cu(phen)_2OAc]^+$ cation, $[\mathbf{3}]^+$, displays a distorted square-pyramidal geometry ($\tau = 0.28$[30]) with an axial N-donor and a κ^1-OAc ligand (Cu–O distances = 2.01 Å/2.70 Å), similar to the cation in the solid state structure of **[3]OAc** ($\tau = 0.42$, Cu–O = 2.00/2.64 Å[23]). A variety of alternative precursor species were also assessed: 6-coordinate $Cu(phen)_2(OAc)_x(X)_{2-x}$ (X = I, OAc; x = 0–2); cationic $[Cu(phen)_2(X)(S)]^+$ (S = MeOH, H_2O) and mono-phen 4-coordinate $Cu(phen)(OAc)_x(I)_{2-x}$ (see ESI for details). Of these the most accessible was $Cu(phen)(OAc)_2$ (ΔG = +3.1 kcal/mol)

while OAc/I exchange in **[3]**$^+$ to give 5-coordinate [Cu(phen)$_2$I]$^+$ (**[5]**$^+$) was endergonic by 5.4 kcal/mol. The computed geometry of **[5]**$^+$ is trigonal bipyramidal ($\tau = 0.90$) in good agreement with the solid-state structure of **[5]I** ($\tau = 0.85$). Similar speciation studies identified [Cu(phen)$_2$Ph]$^+$, **[8]**$^+$, as the most stable Cu-aryl intermediate formed upon transmetalation (where Ph was used as the prototypical aryl group). **[8]**$^+$ exhibits a distorted square-pyramidal geometry with an axial N-donor ($\tau = 0.37$). Cu(phen)$_2$(I)Ph, **9**, lies only 0.8 kcal/mol above **[8]**$^+$ suggesting it would be readily accessible in solution. Loss of a phen ligand from **9** to form Cu(phen)(I)(Ph) is disfavored ($\Delta G = +7.5$ kcal/mol).

Having identified **[3]**$^+$ and **[8]**$^+$ as the most likely precursor and intermediate formed in the transmetalation step, we turned to the details of that process. The most accessible computed profile is shown in Figure 4a, where the acetate present in solution engages **1a** to deliver the cognate boronate.[31] This first binds to **[3]**$^+$ via a hydroxyl substituent to give **Int(3$^+$-8$^+$)1** at +11.5 kcal/mol. Dissociation of the Cu-bound acetate ligand then forms **Int(3$^+$-8$^+$)2** (+7.4 kcal/mol) from which the Cu–N^1 phen arm decoordinates to form **Int(3$^+$-8$^+$)3** (+15.3 kcal/mol), which features a strong H-bond with the Cu-bound OH of the boronate (N^1···H^1 = 1.62 Å, see also Figure 4d for the computed structure and atom labelling). This places the Ph group adjacent to a vacant site at Cu (Cu···C^1 = 2.40 Å) from which Ph group transfer can readily occur via **TS(3$^+$-8$^+$)** with an additional barrier of only 6.6 kcal/mol. All Cu–N bonds lengthen slightly in this transition state to accommodate the transferring phenyl group while the N^1···H^1 shortens further to 1.56 Å. The initial Cu–phenyl intermediate, **Int(3$^+$-8$^+$)4** (+11.1 kcal/mol), retains the B(OH)$_2$(OAc) side-product via Cu–O and OH···N interactions. Dissociation of this species with re-coordination of the free phen arm then forms **[8]**$^+$ at +5.2 kcal/mol. Transmetalation therefore occurs with an accessible overall barrier of 21.9 kcal/mol, but is endergonic by 5.2 kcal/mol. This is consistent with the non-observation of any Cu-aryl species when the reaction is performed in the absence of a halide source.[32]

Retention of the weakly bound κ^1-*N*-phen ligand in **TS(3$^+$-8$^+$)** is important as in its absence the overall barrier for an equivalent mono-phen pathway increases to 34.4 kcal/mol. Alternative transition states were also located in which MeOH or H$_2$O solvent molecules act as H-bond acceptors to the boronate with similar overall computed barriers of 22.0 kcal/mol and 22.8 kcal/mol, respectively. Elongation of the Cu–N^1 distance was far less marked in these cases (ca. 2.53 Å) and IRC calculations indicated direct formation of **[8]**$^+$ with expulsion of AcOB(OH)$_2$ (i.e., no intermediate equivalent to **Int(3$^+$-8$^+$)4** was located). Other pathways, including those in which HO$^-$ was considered as base, proved higher in energy; in addition, transmetalation with PhBpin gave a higher overall barrier of 26.9 kcal/mol (see ESI for full details).

Once **[8]**$^+$ is formed, iodide can readily add to give Cu(phen)$_2$(Ph)(I), **9** from which reductive elimination of PhI could in principle occur. However, this process would form a Cu(0) species and was shown to be thermodynamically inaccessible ($\Delta G = +18.1$ kcal/mol). Instead we propose **9** undergoes disproportionation with a further equivalent of **[3]**$^+$ to form Cu(I) species [Cu(phen)$_2$]$^+$, **[10]**$^+$, and a Cu(III) species, Cu(phen)(I)(OAc)Ph, **11** (Figure 4b).

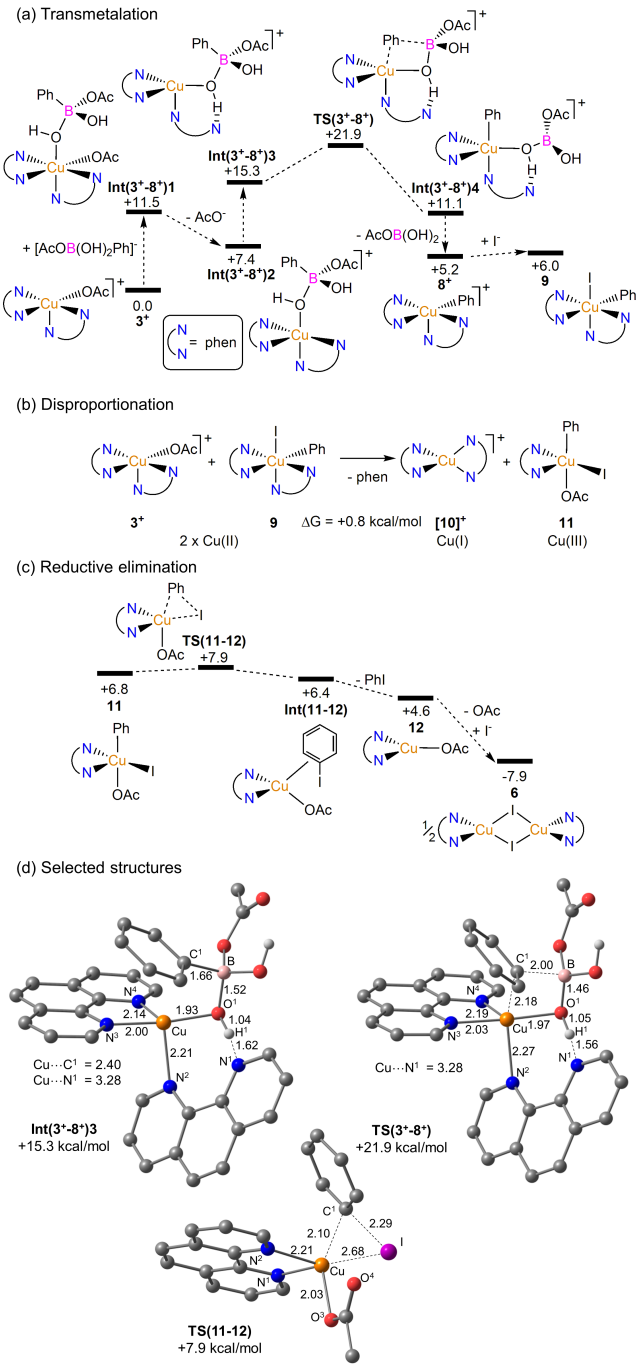

Figure 4. Computed reaction profiles (free energies, kcal/mol) for: (a) The transmetalation step linking [3]$^+$ to [8]$^+$ and 9 with AcO$^-$ as base; (b) Disproportionation of Cu(II) intermediates [3]$^+$ and 9; and (c) Reductive elimination from Cu(III) intermediate 11. (d) Selected computed geometries with key distances in Å and non-hydroxy H atoms omitted for clarity. See ESI for alternative pathways considered.

11 is the lowest of four low-spin square-pyramidal Cu(III) isomers that all lie with 4 kcal/mol; all these structures are at least 17 kcal/mol less stable when computed as a high-spin triplet. Ph–I bond forming reductive elimination from **11** then proceeds with a minimal barrier of 1.1 kcal/mol to form an initial η^2-PhI complex at +10.5 kcal/mol (see Figure 4c). Dissociation of the

https://doi.org/10.26434/chemrxiv-2023-kl7tr-v2 **ORCID:** https://orcid.org/0000-0002-1582-4286

PhI product forms Cu(phen)(OAc), **12**, at which AcO^-/I^- substitution and dimerization yields $[Cu(\mu\text{-}I)(phen)]_2$ **6**, at –7.9 kcal/mol.

The DFT modelling studies indicate that bis-phen species are implicated both prior to ($[\mathbf{3}]^+$) and after ($[\mathbf{8}]^+$) the transmetalation step and that it is the disproportionation step that forms a mono-phen Cu(III) intermediate, **11**. Both the transmetalation and the disproportionation steps are slightly endergonic, but the kinetically facile Ph–I reductive elimination from **11** drives the reaction to completion once coupled with the thermodynamically favorable formation of Cu(I) dimer **6**. The $AcOB(OH)_2$ side-product formed in the computed mechanism would be readily hydrolyzed under the reaction conditions releasing AcOH. AcOH facilitates the Cu(I) oxidative turnover step with O_2 to re-form $[\mathbf{3}]^+$ (see Figure 3)[15-17] and releasing AcO^-, which is then available for the boronate formation that enables the transmetalation step under catalytic turnover.

Based on the totality of the dataset, an illustrative description of the proposed key events of the catalytic cycle is provided in Scheme 5.

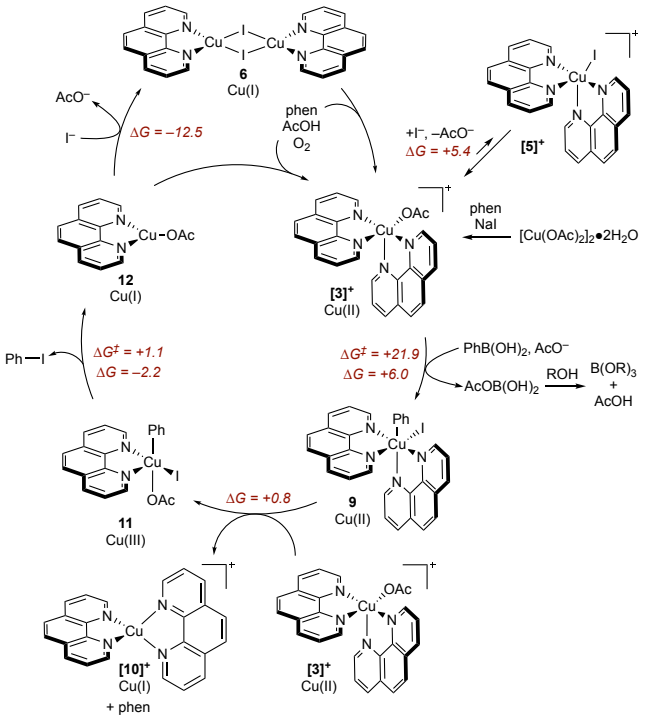

Scheme 5. Proposed catalytic cycle with computed free energy changes and activation barriers (kcal/mol) shown in italics.

$[Cu(OAc)_2]_2\bullet 2H_2O$ undergoes denucleation in the presence of phen and NaI to give $[\mathbf{3}]^+$. $[\mathbf{5}]^+$ can, in principle, be accessed from $[\mathbf{3}]^+$, but the equilibrium is negligible. AcO^- induces boronate formation from the arylboronic acid, facilitating transmetalation to give initially $\mathbf{8}^+$ that then adds I^- to form **9**. Disproportionation of **9** and $[\mathbf{3}]^+$ gives Cu(III) complex **11** along with Cu(I) species $[\mathbf{10}]^+$, and so proceeds with loss of one phen ligand. **11** then undergoes reductive elimination, delivering the aryl iodide product and Cu(I) species **12**. Anion metathesis of **12** delivers Cu(I) dimer **6**, which undergoes oxidative turnover by action of AcOH and O_2 in the presence of phen, to close the catalytic cycle.

In summary, a combination of experimental and computational investigations has provided the first complete description of the Cu-catalyzed iododeboronation reaction. This analysis has revealed the key role of the ligand in three critical steps – facilitating transmetalation via H-bonding to the boronate and promoting the key oxidative events (disproportionation and turnover). More specifically, ligand speciation is a key operation – ligand loss is required at disproportionation, but gain is required at oxidative turnover, which provides a basis for understanding of ligand stoichiometry. These data therefore add to the wider knowledge base of Cu-mediated oxidative coupling reactions and may support understanding and development of related processes, including the related fluorodeboronation reaction.

ASSOCIATED CONTENT

Data Availability Statement

The research data supporting this publication can be accessed at https://doi.org/10.17630/8603890e-da81-4225-9343-a3f5baba470c. Crystallographic data for compounds **[3]OAc**, **[3]Cl**, **4**, **5**, and **6** is available from the Cambridge Crystallographic Data Centre (CCDC) under Deposition Numbers 2258899–2258903.

Supporting Information

Experimental procedures, characterization data, computational data, x-ray data. Supporting Information is available free of charge on the ACS Publications website.

AUTHOR INFORMATION

Corresponding Author

* s.a.macgregor@hw.ac.uk
* aw260@st-andrews.ac.uk

Author Contributions

All authors have given approval to the final version of the manuscript.
‡These authors contributed equally.

Funding Sources

Engineering and Physical Sciences Research Council (EPSRC) grant no. EP/R025754/1, EP/S027165/1, EP/W007517/1.
Biotechnology and Biological Sciences Research Council (BBSRC) grant BB/R013780/1.
Leverhulme Trust grant no. RF-2022-014

Notes

Any additional relevant notes should be placed here.

ACKNOWLEDGMENT

We thank Suzie Davison for help with control experiments. A.J.B.W. thanks the Leverhulme Trust for a Research Fellowship and the EPSRC Programme Grant "Boron: Beyond the Reagent" for support. We thank Dr Bela E. Bode for assistance with EPR measurements and Heriot-Watt University for a James Watt Scholarship to A.C.

ABBREVIATIONS

Ac, acyl; Ar, aryl; IRC, intrinsic reaction coordinate; phen, 1,10-phenanthroline; Ph, phenyl; pin, pinacolato.

REFERENCES

(1) Zhang, G.; Lv, G.; Li, L.; Chen, F.; Cheng, J. Copper-catalyzed halogenation of arylboronic acids. *Tetrahedron Lett.* **2011**, *52*, 1993–1995.

(2) Yang, H.; Li, Y.; Jiang. M.; Wang, J.; Fu, H. General copper-catalyzed transformations of functional groups from arylboronic acids in water. *Chem. Eur. J.* **2011**, *17*, 5652–5660.
(3) Sterically controlled iodination of arenes via iridium-catalyzed C–H borylation. Partridge, B. M.; Hartwig, J. F. *Org. Lett.* **2013**, *15*, 140–143.
(4) Tale, R. H.; Toradmal, G. K.; Gopula, V. B. A practical and general ipso iodination of arylboronic acids using N-iodomorpholinium iodide (NIMI) as a novel iodinating agent: mild and regioselective synthesis of aryliodides. *RSC Adv.* **2015**, *5*, 84910–84919.
(5) Heindel, N. D.; Burns, H. D.; Honda, T.; Brady, L. W. *The Chemistry of Radiopharmaceuticals.* Mayson: New York, 1978.
(6) Zhang, P.; Zhuang, R.; Guo, Z.; Su, X.; Chen, X.; Zhang, X. A highly efficient copper-mediated radioiodination approach using aryl boronic acids. *Chem. Eur. J.* **2016**, *22*, 16783–16786.
(7) Radiosynthesis of SPECT tracers via a copper mediated ^{123}I iodination of (hetero)aryl boron reagents. Wilson, T. C.; McSweeney, G.; Preshlock, S.; Verhoog, S.; Tredwell, M.; Cailly, T.; Gouverneur, V. *Chem. Commun.* **2016**, *52*, 13277–13280.
(8) Reilly, S. W.; Makvandi, M.; Kuiying Xu, K.; Mach, R. H. Rapid Cu-catalyzed [^{211}At]astatination and [^{125}I]iodination of boronic esters at room temperature. *Org. Lett.* **2018**, *20*, 1752–1755.
(9) Wilson, T. C. Late Stage ^{18}F-fluorination and ^{123}I- iodination for PET and SPECT imaging. PhD Thesis, University of Oxford, **2018**. https://ora.ox.ac.uk/objects/uuid:a6c1513e-9945-42d0-8e0a-176a49f0d653/download_file?file_format=application%2Fpdf&safe_filename=TW%2BFinal%2BThesis.pdf&type_of_work=Thesis
(10) Dong, T.; Tsui, G. C. Construction of carbon-fluorine bonds via copper-catalyzed/-mediated fluorination reactions. *Chem. Rec.* **2021**, *21*, 4015– 4031.
(11) Fier, P. S.; Luo, J.; Hartwig, J. F. Copper-mediated fluorination of arylboronate esters. Identification of a copper(III) fluoride complex. *J. Am. Chem. Soc.* **2013**, *135*, 2552–2559.
(12) Ye, Y.; Sanford, M. S. Mild Copper-mediated fluorination of aryl stannanes and aryl trifluoroborates. *J. Am. Chem. Soc.* **2013**, *135*, 4648−4651.
(13) Tredwell, M.; Preshlock, S. M.; Taylor, N. J.; Gruber, S.; Huiban, M.; Passchier, J.; Mercier, J.; Génicot, C.; Gouverneur, V. A general copper-mediated nucleophilic ^{18}F fluorination of arenes. *Angew. Chem. Int. Ed.* **2014**, *53*, 7751–7755.
(14) West, M. J.; Fyfe, J. W. B.; Vantourout, J. C.; Watson, A. J. B. Mechanistic development and recent applications of the Chan–Lam amination. *Chem. Rev.* **2019**, *119*, 12491–12523.
(15) King, A. E.; Ryland, B. L.; Brunold, T. C.; Stahl, S. S. Kinetic and spectroscopic studies of aerobic copper(II)-catalyzed methoxylation of arylboronic esters and insights into aryl transmetalation to copper(II). *Organometallics* **2012**, *31*, 7948– 7957.
(16) King, A. E.; Brunold, T. C.; Stahl, S. S. Mechanistic study of copper-catalyzed aerobic oxidative coupling of arylboronic esters and methanol: Insights into an organometallic oxidase reaction. *J. Am. Chem. Soc.* **2009**, *131*, 5044– 5045.
(17) Vantourout, J. C.; Miras, H. N.; Isidro-Llobet, A.; Sproules, S.; Watson, A. J. B. Spectroscopic studies of the Chan–Lam amination: A mechanism-inspired solution to boronic ester reactivity. *J. Am. Chem. Soc.* **2017**, *139*, 4769– 4779.
(18) Vantourout, J. C.; Li, L.; Bendito-Moll, E.; Chabbra, S.; Arrington, K.; Bode, B. E.; Isidro-Llobet, A.; Kowalski, J. A.; Nilson, M.; Wheelhouse, K.; Woodward, J. L.; Xie, S.; Leitch, D. C.; Watson, A. J. B. Mechanistic insight enables practical, scalable, room temperature Chan-Lam N-arylation of N-aryl sulfonamides. *ACS Catal.* **2018**, *8*, 9560–9566.
(19) Hardouin Duparc, V.; Schaper, F. Sulfonato-diketimine copper(II) complexes: Synthesis and application as catalysts in Chan–Evans–Lam couplings. *Organometallics* **2017**, *36*, 3053– 3060.
(20) Hardouin Duparc, V.; Bano, G. L.; Schaper, F. Chan–Evans–Lam couplings with copper iminoarylsulfonate complexes: Scope and mechanism. *ACS Catal.* **2018**, *8*, 7308–7325.
(21) For stoichiometric Cu(III) complexes relevant to Chan–Lam chemistry, see: (a) Ribas, X.; Jackson, D. A.; Donnadieu, B.; Mahía, J.; Parella, T.; Xifra, R.; Hedman, B.; Hodgson, K. O.; Llobet, A.; Stack, T. D. P. Aryl C−H activation by Cu(II) to form an organometallic aryl−Cu(III) species: A novel twist on copper disproportionation. *Angew. Chem. Int. Ed.* **2002**, *41*, 2991−2994. (b) Xifra, R.; Ribas, X.; Llobet, A.; Poater, A.; Duran, M.; Solà, M.; Stack, T. D. P.; Benet-Buchholz, J.; Donnadieu, B.; Mahía, J.; Parella, T. Fine-tuning the electronic properties of highly stable organometallic Cu^{III} complexes containing monoanionic macrocyclic ligands. *Chem. Eur. J.* **2005**, *11*, 5146−5156.
(22) Bose, S.; Dutta, S.; Koley, D. Entering chemical space with theoretical underpinning of the mechanistic pathways in the Chan–Lam amination. *ACS Catal.* **2022**, *12*, 1461–1474.
(23) Jing, B.; Li, L.; Dong, J.; Xu, T. (Acetato-κ*O*)bis(1,10-phenanthroline-κ^2*N*,*N*')copper(II) acetate heptahydrate. *Acta Cryst.* **2011**. *E67*, m464.
(24) Devereux, M.; O'Shea, D.; O'Connor, M.; Grehan, H.; Connor, G.; McCann, M.; Rosair, G.; Lyng, F.; Kellett, A.; Walsh, M.; Egan, D.; Thati, B. Synthesis, catalase, superoxide dismutase and antitumour activities of copper(II) carboxylate complexes incorporating benzimidazole, 1,10-phenanthroline and bipyridine ligands: X-ray crystal structures of $[Cu(BZA)_2(bipy)(H_2O)]$, $[Cu(SalH)_2(BZDH)_2]$ and $[Cu(CH_3COO)_2(5,6\text{-}DMBZDH)_2]$ ($SalH_2$ = salicylic acid; BZAH = benzoic acid; BZDH = benzimidazole and 5,6-DMBZDH = 5,6-dimethylbenzimidazole). *Polyhedron* **2007**, *26*, 4073–4084.
(25) Nagle, P.; Hathaway, B. J. Structure of iodobis(1,10-phenanthroline)copper(II) iodide monohydrate. *Acta Cryst.* **1991**, *C47*, 1386–1389.
(26) Yu, J.-H.; Lü, Z.-L.; Xu, J.-Q.; Bie, H.-Y.; Lu, J.; Zhang, X. Synthesis, characterization and optical properties of some copper(I) halides with 1,10-phenanthroline ligand. *New J. Chem.* **2004**, *28*, 940–945.
(27) Seco, J. M.; Quirós, M.; González Garmendia, M. J. Synthesis, X-ray crystal structure and spectroscopic, magnetic and EPR studies of Cu(II) dimers with methoxy-di-2-pyridyl)methoxide as bridging ligand. *Polyhedron* **2000**, *19*, 1005–1013.
(28) Latham, K.; Mensforth, E. J.; Rixa, C. J.; White, J. M. Synthesis of supramolecular metallo-amine-oxy acid systems via crystal disassembly/reassembly. *CrystEngComm.* **2009**, *11*, 1343–1351.
(29) DFT calculations employed Gaussian16 with geometries optimized with the BP86 functional including methanol solvent through the PCM approach. An SDD pseudopotential and basis set was employed for Cu and 6-31g** for all other atoms. Electronic energies were corrected for dispersion (BJD3) and basis set effects (def2tzvp) and combined with the thermochemical corrections from the initial optimizations to give the free energies in the text. See ESI for full details and references.
(30) Addison, W.; Rao, T. N.; Reedijk, J.; van Rijn, J.; Verschoor, G. C. Synthesis, structure, and spectroscopic properties of copper(II) compounds containing nitrogen–sulphur donor ligands; The crystal and molecular structure of aqua[1,7-bis(*N*-methylbenzimidazol-2′-yl)-2,6-dithiaheptane]copper(II) perchlorate. *J. Chem. Soc., Dalton Trans.* **1984**, *1984*, 1349–1356.
(31) Molloy, J. J.; O'Rourke, K. M.; Frias, C. P.; Sloan, N.; West, M. J.; Pimlott, S. L.; Sutherland, A.; Watson, A. J. B. Mechanism of Cu-catalyzed aryl boronic acid halodeboronation using electrophilic halogen: Development of a base-catalyzed iododeboronation for radiolabeling applications. *Org. Lett.* **2019**, *21*, 2488−2492.
(32) In contrast, Koley and co-workers in their study of the Chan–Lam reaction found the rate-limiting transition state corresponded to reductive elimination (see ref 22). In that study the B3LYP functional was employed. Accordingly, to assess any

functional dependency, we recomputed our results with B3LYP and found that transmetalation remains rate-limiting.

Table of Contents artwork

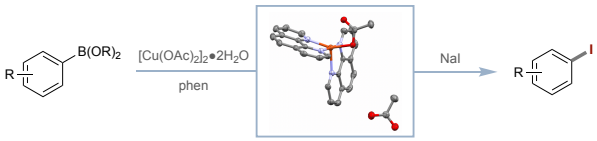

active catalyst species identified • ligand-controlled transmetalation • turnover events rationalized